Chiral effective field theory calculations of neutrino processes in dense matter

S. Bacca,[1,*] K. Hally,[1,2,†] C. J. Pethick,[3,4,‡] and A. Schwenk[1,§]

[1] TRIUMF, 4004 Wesbrook Mall, Vancouver, BC, V6T 2A3, Canada
[2] Acadia University, Department of Physics, P.O. Box 49, Wolfville, Nova Scotia, B4P 2R6, Canada
[3] The Niels Bohr Institute, Blegdamsvej 17, DK-2100 Copenhagen Ø, Denmark
[4] NORDITA, Roslagstullsbacken 21, 10691 Stockholm, Sweden

We calculate neutrino processes involving two nucleons at subnuclear densities using chiral effective field theory. Shorter-range noncentral forces reduce the neutrino rates significantly compared with the one-pion exchange approximation currently used in supernova simulations. For densities $\rho < 10^{14}\,\mathrm{g\,cm^{-3}}$, we find that neutrino rates are well constrained by nuclear interactions and nucleon-nucleon scattering data. As an application, we calculate the mean-square energy transfer in scattering of a neutrino from nucleons and find that collision processes and spin-dependent mean-field effects dominate over the energy transfer due to nucleon recoil.

PACS numbers: 97.60.Bw, 26.50.+x, 95.30.Cq, 26.60.-c

Neutrino processes involving two nucleons (NN) play a special role in the physics of core-collapse supernovae and neutron stars: Neutrino-pair bremsstrahlung and absorption, $NN \leftrightarrow NN\nu\overline{\nu}$, are key for the production of muon and tau neutrinos, for their spectra, and for equilibrating neutrino number densities [1, 2, 3, 4, 5, 6]. Since neutrinos interact weakly, the rates for neutrino emission, absorption and scattering are determined by the dynamic response functions of strongly-interacting matter. Supernova explosions are most sensitive to neutrino processes near the protoneutron star, at subnuclear densities $\rho \lesssim \rho_0/10$ ($\rho_0 = 2.8 \times 10^{14}\,\mathrm{g\,cm^{-3}}$ being the saturation density), and where matter is neutron rich. In this regime, there exist to date no systematic calculations of neutrino rates that go beyond the one-pion exchange (OPE) approximation for the nucleon-nucleon interaction. In this paper, we present first results for neutrino processes in neutron matter based on chiral effective field theory (EFT).

Noncentral contributions to strong interactions, due to tensor forces from pion exchanges and spin-orbit forces, are essential for the two-nucleon response. This follows from direct calculations of neutrino-pair bremsstrahlung [7] and from conservation laws [8]. In supernova and neutron star simulations, the standard rates for bremsstrahlung and absorption are based on the OPE approximation [4, 7]. This is a reasonable starting point, since it represents the long-range part of nuclear forces, and for neutron matter, it is the leading-order contribution in chiral EFT [9]. However, for the relevant Fermi momenta $k_\mathrm{F} \sim 1.0\,\mathrm{fm}^{-1} \approx 200\,\mathrm{MeV}$, subleading noncentral contributions are crucial for reproducing NN scattering data [9]. In this paper, we go beyond the OPE approximation and include contributions up to next-to-next-to-next-to-leading order (N^{3}LO) in chiral EFT. We find that shorter-range noncentral forces significantly reduce the neutrino rates for all relevant densities. As an application, we calculate the mean-square energy transfer in scattering of a neutrino from nucleons and find that collision processes and spin-dependent mean-field effects are more important than nonzero momentum transfers to the nucleons. This establishes that the long-wavelength approximation used in the OPE calculations [4] is reasonable.

We follow the approach to neutrino processes in nucleon matter developed in Ref. [10], which is based on Landau's theory of Fermi liquids and consistently includes one-quasiparticle-quasihole pair states (corresponding to elastic scattering of neutrinos from nucleons) and two-quasiparticle-quasihole pair states, which are taken into account through the collision integral in the Landau transport equation for quasiparticles. Using a relaxation time approximation, the transport equation can be solved and this leads to a general form for the response functions [10]. The spin response includes multiple-scattering effects, thereby taking into account the Landau-Pomeranchuk-Migdal (LPM) effect, and generalizes earlier work to finite wavelengths.

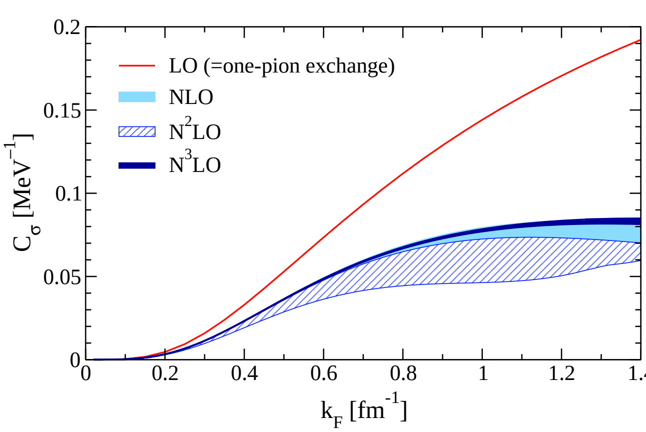

FIG. 1: (Color online) Spin relaxation rate given by C_σ of Eq. (4) as a function of Fermi momentum k_F obtained from chiral EFT interactions of successively higher orders [14]. All results are for $m^*/m = 1$.

Basic formalism. In supernovae and neutron stars, the energy ω and momenta $\mathbf{q}$ transferred by neutrinos to the system are small compared to the momenta of nucleons. In addition, we consider degenerate conditions, where the temperature is small compared to the Fermi energy, $T/\varepsilon_{\rm F} \lesssim 1/3$. This is the regime in which Landau's theory of Fermi liquids is a reasonable first approximation, and includes the conditions under which the two-nucleon response is effective. We focus on axial current processes, since they dominate in many situations and are most affected by NN interactions. The corresponding neutrino rates are given by [1]

$$\Gamma(\omega,\mathbf{q}) = 2\pi\, n\, G_{\rm F}^2\, C_{\rm A}^2\, (3-\cos\theta)\, S_{\rm A}(\omega,\mathbf{q})\,, \tag{1}$$

multiplied by occupation probabilities for the initial neutrino states and Pauli-blocking factors for final states. Here n denotes the neutron number density, $G_{\rm F}$ the Fermi coupling constant, $C_{\rm A} = -g_a/2 = -1.26/2$ the axial-vector coupling for neutrons, and θ is the angle between the initial and final neutrino momenta for scattering, or between the neutrino momentum and minus the antineutrino momentum for neutrino-pair bremsstrahlung and absorption. The axial or spin dynamical structure factor $S_{\rm A}$ is given by [11]

$$S_{\rm A}(\omega,\mathbf{q}) = \frac{1}{\pi n}\,\frac{1}{1-e^{-\omega/T}}\,{\rm Im}\,\chi_\sigma(\omega,\mathbf{q})\,, \tag{2}$$

where χ_σ is the spin-density–spin-density response function, and we use units with $\hbar = c = k_{\rm B} = 1$. The solution [10] to the Landau transport equation leads to $\chi_\sigma = N(0)\,\widetilde{X}_\sigma/(1+G_0\widetilde{X}_\sigma)$, with density of states at the Fermi surface $N(0) = m^* k_{\rm F}/\pi^2$, nucleon effective mass m^*, and Landau parameter G_0 for the spin-dependent part of the interaction. In the relaxation time approximation, the response function $\widetilde{X}_\sigma$ (for $G_0 = 0$) is

$$\widetilde{X}_\sigma = 1 - \frac{\omega}{2 v_{\rm F} q}\ln\!\left(\frac{\omega + i/\tau_\sigma + v_{\rm F} q}{\omega + i/\tau_\sigma - v_{\rm F} q}\right), \tag{3}$$

where τ_σ denotes the spin relaxation time and $v_{\rm F} = k_{\rm F}/m^*$ is the Fermi velocity. For frequencies $|\omega| \gg 1/\tau_\sigma$ and $q \ll k_{\rm F}$, the spin relaxation rate is given by [10, 12]

$$\frac{1}{\tau_\sigma} = C_\sigma\left[T^2 + (\omega/2\pi)^2\right] \quad \text{with} \quad C_\sigma = \frac{\pi^3 m^*}{6k_{\rm F}^2}\left\langle \frac{1}{12}\sum_{k=1,2,3}{\rm Tr}\Big[\mathcal{A}_{\boldsymbol{\sigma}_1,\boldsymbol{\sigma}_2}(\mathbf{k},\mathbf{k}')\,\boldsymbol{\sigma}_1^k\left[(\boldsymbol{\sigma}_1+\boldsymbol{\sigma}_2)^k\,,\,\mathcal{A}_{\boldsymbol{\sigma}_1,\boldsymbol{\sigma}_2}(-\mathbf{k},\mathbf{k}')\right]\Big]\right\rangle, \tag{4}$$

where $\mathcal{A}_{\boldsymbol{\sigma}_1,\boldsymbol{\sigma}_2}(\mathbf{k},\mathbf{k}')$ is the quasiparticle scattering amplitude multiplied by $N(0)$, $\mathbf{k} = \mathbf{p}_1 - \mathbf{p}_3$ and $\mathbf{k}' = \mathbf{p}_1 - \mathbf{p}_4$ are the nucleon momentum transfers, and the average $\langle \ldots \rangle$ is over the Fermi surface (for details see [10]). The commutator with the two-body spin operator demonstrates that only noncentral interactions contribute.

We treat the strong interaction in Born approximation and evaluate the spin trace for C_σ in two-body spin space $|s\, m_s\rangle$ using a partial-wave expansion. For $s=0$ the spin trace vanishes, thus only $s=1$ states and odd orbital angular momenta $\ell, \ell', \tilde{\ell}, \tilde{\ell}'$ contribute, and we find

$$\begin{aligned} C_\sigma = \frac{16\pi m^{*3}}{9k_{\rm F}} \sum_{j\ell\ell'}\sum_{\tilde{j}\tilde{\ell}\tilde{\ell}'}\sum_{L}\sum_{J={\rm even}}\sum_{m_s m_s'} i^{\ell-\ell'+\tilde{\ell}'-\tilde{\ell}}\,(-1)^{j+\tilde{j}+L}\,\big(\widehat{j}\,\widehat{\tilde{j}}\,\widehat{L}\,\widehat{J}\big)^2\,\widehat{\ell}\,\widehat{\ell'}\,\widehat{\tilde{\ell}}\,\widehat{\tilde{\ell}'}\left[\frac{J!}{2^J\,(J/2)!^2}\right]^2 \begin{pmatrix} \ell & \tilde{\ell} & J \\ 0 & 0 & 0 \end{pmatrix}\begin{pmatrix} \ell' & \tilde{\ell}' & J \\ 0 & 0 & 0 \end{pmatrix} \\ \times \begin{Bmatrix} \ell & \ell' & L \\ 1 & 1 & j \end{Bmatrix}\begin{Bmatrix} \tilde{\ell}' & \tilde{\ell} & L \\ 1 & 1 & \tilde{j} \end{Bmatrix}\begin{Bmatrix} \ell' & \ell & L \\ \tilde{\ell} & \tilde{\ell}' & J \end{Bmatrix}\left[\mathcal{C}^{1m_s}_{L(m_s-m_s')1m_s'}\right]^2 (m_s^2 - m_s m_s')\int_0^{k_{\rm F}}\frac{p\,dp}{\sqrt{k_{\rm F}^2-p^2}}\,\langle p|V^{js=1}_{\ell'\ell}|p\rangle\langle p|V^{\tilde{j}s=1}_{\tilde{\ell}\tilde{\ell}'}|p\rangle\,, \end{aligned} \tag{5}$$

where $j, \tilde{j}$ are total angular momenta, p is the magnitude of the relative momenta $p = |\mathbf{p}_1 - \mathbf{p}_2|/2 = |\mathbf{p}_3 - \mathbf{p}_4|/2$, and $\langle p|V^{js}_{\ell'\ell}|p\rangle$ are partial-wave matrix elements of the strong interaction. We use $\widehat{a} = \sqrt{2a+1}$ and standard notation for Clebsch-Gordan, $3j$ and $6j$ symbols [13].

Results. In Fig. 1, we show the spin relaxation rate calculated from chiral EFT interactions up to N^{3}LO as a function of the Fermi momentum over a wide density range ($k_{\rm F} = 1.4\,{\rm fm}^{-1}$ corresponds to $\rho = m k_{\rm F}^3/(3\pi^2) = 1.6\times 10^{14}\,{\rm g\,cm}^{-3}$) [23]. The neutrino-pair bremsstrahlung and absorption rates are proportional to C_σ to a good approximation when $|\omega| \gg 1/\tau_\sigma$, while for larger val-

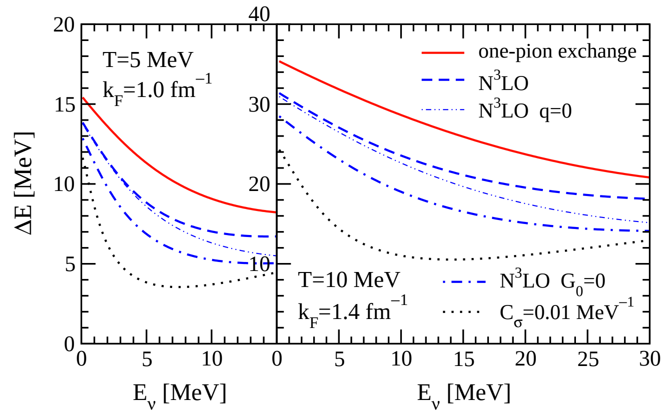

FIG. 2: (Color online) The rms energy transfer ΔE in neutrino scattering from neutrons as a function of initial neutrino energy E_ν for two T-$k_{\rm F}$ combinations. Results are shown for different C_σ (OPE, N^{3}LO using Eq. (9), and a lower value), in the long-wavelength limit ($q=0$), all with $G_0=0.8$ [16], and in the absence of mean-field effects ($G_0=0$).

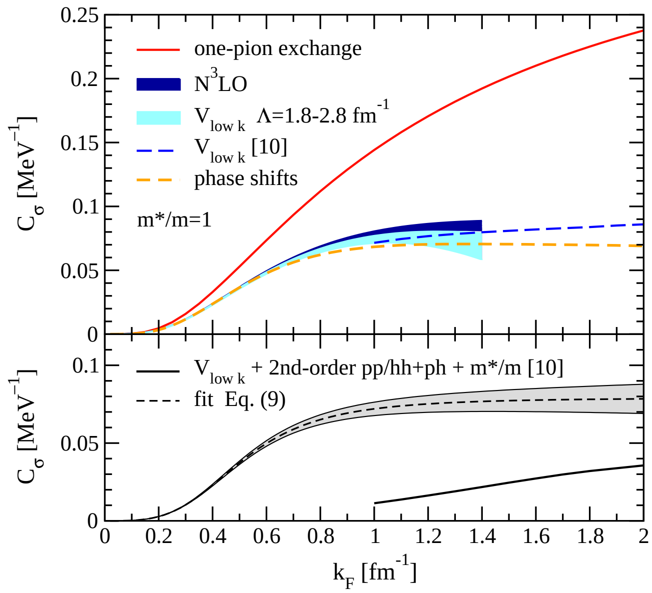

FIG. 3: (Color online) Combined results for the spin relaxation rate given by C_σ: bands for different chiral N^{3}LO potentials [14, 15] and chiral $V_{{\rm low}\,k}$ interactions [17] and the result based on phase shifts. We also include the rate of Ref. [10] for $V_{{\rm low}\,k}$ with a density-dependent cutoff $\Lambda=\sqrt{2}\,k_{\rm F}$. All results are for $m^*/m=1$ (also for Ref. [10]). Lower panel: The band represents the C_σ range in the upper panel based on nuclear interactions and NN phase shifts. The solid line includes second-order many-body and m^* contributions, with $m^*/m \approx 1.12-0.17\,(k_{\rm F}/\,{\rm fm}^{-1})$ over this range [10].

ues of C_σ they are suppressed by the LPM effect [1, 10]. The leading order (LO) contribution includes OPE as the only noncentral interaction, which provides the standard two-nucleon rates used in current supernova simulations. Our results based on chiral EFT interactions of successively higher orders of Epelbaum *et al.* (EGM) [14] show that OPE significantly overestimates C_σ for all relevant densities. The bands at next-to-leading order (NLO), N^{2}LO, and N^{3}LO provide an estimate of the theoretical uncertainty, generated by varying the cutoff Λ as well as a spectral function cutoff in the irreducible 2π-exchange $\Lambda_{\rm SF}$ [9, 14]. Chiral EFT interactions at N^{3}LO accurately reproduce low-energy NN scattering [14, 15], and at this order, C_σ is practically independent of the N^{3}LO potential for these densities. Most of the reduction of C_σ occurs at the NLO level, which includes the leading 2π-exchange tensor force (for $\Lambda_{\rm SF}\to\infty$)

$$V_{2\pi,\,{\rm t}}^{\rm NLO} = -\,\boldsymbol{\sigma}_1\cdot\mathbf{k}\,\boldsymbol{\sigma}_2\cdot\mathbf{k}\,\frac{3\,w\,g_a^4}{64\,k\,\pi^2F_\pi^4}\,\ln\frac{w+k}{2m_\pi}\,, \qquad (6)$$

and shorter-range noncentral contact interactions

$$V_{C,\,{\rm nc}}^{\rm NLO} = \widetilde{C}_1\,\boldsymbol{\sigma}_1\cdot\mathbf{k}\,\boldsymbol{\sigma}_2\cdot\mathbf{k}+\widetilde{C}_2\,\boldsymbol{\sigma}_1\cdot\mathbf{k}'\,\boldsymbol{\sigma}_2\cdot\mathbf{k}' + \widetilde{C}_3\,i\,(\boldsymbol{\sigma}_1-\boldsymbol{\sigma}_2)\cdot(\mathbf{k}\times\mathbf{k}')\,, \qquad (7)$$

where $w=\sqrt{4m_\pi^2+k^2}$ and $\widetilde{C}_i$ are constrained by NN scattering data (S- and P-waves). $V_{2\pi,\,{\rm t}}^{\rm NLO}$ added to OPE increases C_σ (to $0.29\,{\rm MeV}^{-1}$ at $k_{\rm F}=1.0\,{\rm fm}^{-1}$), but this is compensated by the repulsive shorter-range $V_{C,\,{\rm nc}}^{\rm NLO}$.

Energy transfer. Figure 2 shows the impact of C_σ on the root-mean-square (rms) energy transfer ΔE in scattering from nucleons. In the absence of Pauli blocking of final neutrino states, ΔE is given by

$$(\Delta E)^2 = \frac{\int d\mathbf{p}'_\nu\,(E_\nu-E'_\nu)^2\,\Gamma(E_\nu-E'_\nu,p_\nu-p'_\nu)}{\int d\mathbf{p}'_\nu\,\Gamma(E_\nu-E'_\nu,p_\nu-p'_\nu)}\,. \qquad (8)$$

For the N^{3}LO results, the comparison with the long-wavelength approximation ($q=0$) shows that the energy transfer due to nucleon recoil is small. Collision processes are the major contributor to the energy transfer. This is also clear from the decreased ΔE with the lower C_σ value. In addition, the comparison with the $G_0=0$ results demonstrates the increased energy transfer due to repulsive mean-field effects in the spin channel.

Comparison of interactions. We have also carried out calculations for the Entem and Machleidt (EM) N^{3}LO potentials with $\Lambda=500$ and $600\,{\rm MeV}$ [15]. The EM 500 MeV results overlap with the EGM N^{3}LO band of Fig. 1. The EM 600 MeV rate is larger due to the failure of the Born approximation in this case. We have also used the renormalization group (RG) [17] to evolve all N^{3}LO [14, 15] potentials to low-momentum interactions $V_{{\rm low}\,k}$ with $\Lambda=1.8$–$2.8\,{\rm fm}^{-1}$ (360–560 MeV) to extend the estimate of the theoretical uncertainty. The RG preserves the long-range pion exchanges and includes subleading contact interactions, so that NN scattering data are reproduced. The resulting C_σ band is shown in the

upper panel of Fig. 3. This includes the rate based on the evolved EM 600 MeV potential.

In the low-density limit, two-nucleon collisions dominate and NN phase shifts provide a model-independent result for the spin relaxation rate. In the near-degenerate case, the strong potential V in Eq. (5) is then replaced by the free-space K matrix, since Pauli blocking removes the imaginary parts from the loop integrals in the T-matrix equation. We use the standard expression of the K matrix in terms of empirical phase shifts and mixing angles [18] from the Nijmegen Partial Wave analysis (nn-online.org). In general, it is however unclear whether an expansion in terms of the free-space K matrix (or the T matrix) is reliable for $k_{\rm F} \gtrsim 0.1\,{\rm fm}^{-1}$ due to large scattering lengths and Pauli blocking for near-degenerate conditions, unless the relevant parts of V are perturbative. Neutrino-pair bremsstrahlung neglecting mean-field and LPM effects has been calculated from the T matrix in Ref. [19]. For all densities in Fig. 3, we find the striking result that the chiral EFT and $V_{{\rm low}\,k}$ rates obtained in Born approximation are close to those from phase shifts (with the K matrix). This demonstrates that, for these lower cutoffs, the noncentral part of the neutron-neutron amplitude is perturbative in the particle-particle channel.

The upper panel of Fig. 3 combines our results based on nuclear interactions and NN phase shifts, and also includes rates from $V_{{\rm low}\,k}$ interactions [10] that extend to higher densities. At subnuclear densities $\rho < 10^{14}\,{\rm g\,cm}^{-3}$ ($k_{\rm F} < 1.2\,{\rm fm}^{-1}$), the spin response is well constrained and all results lie within a band, with a significantly reduced C_σ compared to OPE. For $k_{\rm F} \gtrsim 1.5\,{\rm fm}^{-1}$, calculations of the equation of state show that low-momentum 3N interactions become important [20] and should be included. In the lower panel of Fig. 3, we show a simple fit representing our results,

$$\frac{C_\sigma}{\rm MeV} = \frac{0.86\,(k_{\rm F}/{\rm fm}^{-1})^{3.6}}{1+10.9\,(k_{\rm F}/{\rm fm}^{-1})^{3.6}}\,, \tag{9}$$

that, together with the spin response function given by Eqs. (2) and (3), can be used in astrophysical simulations.

Many-body effects. Our results above do not include the effects of the nuclear medium on collisions. To give a sense of how these affect C_σ, we show in the lower panel of Fig. 3 rates that include second-order many-body contributions (particle-particle/hole-hole and particle-hole) and self-energy effects through the effective mass m^* (according to Eq. (5), $C_\sigma \sim m^{*\,3}$) [10]. Both particle-hole and m^* effects reduce the spin relaxation rate. The former is driven by second-order particle-hole mixing of tensor with strong central interactions [21]. This demonstrates the need to study in greater detail the influence of many-body effects on collisions (see also Ref. [22]).

In summary, we have presented the first calculations of neutrino processes in supernovae based on chiral EFT. Our N^{3}LO results over the important density range $\rho \lesssim 10^{14}\,{\rm g\,cm}^{-3}$ represent a significant advance beyond the OPE rates currently used in simulations. Shorter-range noncentral forces reduce the rates significantly. For densities $\rho < 10^{14}\,{\rm g\,cm}^{-3}$, the spin response is well constrained by nuclear interactions and NN scattering data. Future work will include neutron-proton mixtures and charged currents, to systematically improve the neutrino physics input for astrophysics.

We thank S. Bogner, M. Liebendörfer, and A. Nogga for useful discussions, and the Niels Bohr International Academy and NORDITA for their hospitality. This work was supported in part by NSERC and the NRC Canada.

* E-mail: bacca@triumf.ca
† E-mail: 079203h@acadiau.ca
‡ E-mail: pethick@nbi.dk
§ E-mail: schwenk@triumf.ca

[1] G. G. Raffelt, *Stars as Laboratories for Fundamental Physics* (University of Chicago Press, 1996).
[2] H. Suzuki, Num. Astrophys. Japan **2**, 267 (1991); in *Proc. International Symp. on Neutrino Astrophys., Frontiers of Neutrino Astrophysics*, ed. Y. Suzuki and K. Nakamura (Tokyo, Universal Academy Press, 1993).
[3] H.-T. Janka, W. Keil, G. Raffelt, and D. Seckel, Phys. Rev. Lett. **76**, 2621 (1996).
[4] S. Hannestad and G. Raffelt, Astrophys. J. **507**, 339 (1998).
[5] T. A. Thompson, A. Burrows, and J. E. Horvath, Phys. Rev. C **62**, 035802 (2000).
[6] M. T. Keil, G. Raffelt, and H.-T. Janka, Astrophys. J. **590**, 971 (2003).
[7] B. Friman and O. V. Maxwell, Astrophys. J. **232**, 541 (1979).
[8] E. Olsson and C. J. Pethick, Phys. Rev. C **66**, 065803 (2002).
[9] For a review of chiral EFT for nuclear forces, see E. Epelbaum, Prog. Part. Nucl. Phys. **57**, 654 (2006).
[10] G. I. Lykasov, C. J. Pethick, and A. Schwenk, Phys. Rev. C **78**, 045803 (2008).
[11] N. Iwamoto and C. J. Pethick, Phys. Rev. D **25**, 313 (1982).
[12] G. I. Lykasov, E. Olsson, and C. J. Pethick, Phys. Rev. C **72**, 025805 (2005).
[13] D. A. Varshalovich, A. N. Moskalev, and V. K. Khersonskii, *Quantum Theory of Angular Momentum* (World Scientific, 1988).
[14] E. Epelbaum, W. Glöckle, and U.-G. Meißner, Nucl. Phys. A **747**, 362 (2005).
[15] D. R. Entem and R. Machleidt, Phys. Rev. C **C68**, 041001(R) (2003).
[16] A. Schwenk, B. Friman, and G. E. Brown, Nucl. Phys. A **713**, 191 (2003).
[17] S. K. Bogner, T. T. S. Kuo, and A. Schwenk, Phys. Rep. **386**, 1 (2003); S. K. Bogner, R. J. Furnstahl, S. Ramanan, and A. Schwenk, Nucl. Phys. A **784**, 79 (2007).
[18] G. E. Brown and A. D. Jackson, *The Nucleon-Nucleon Interaction* (North-Holland Amsterdam, 1976).
[19] C. Hanhart, D. R. Philips, and S. Reddy, Phys. Lett. B **499**, 9 (2001).

[20] L. Tolos, B. Friman, and A. Schwenk, Nucl. Phys. A **806**, 105 (2008).

[21] A. Schwenk and B. Friman, Phys. Rev. Lett. **92**, 082501 (2004); A. Schwenk, P. Jaikumar, and C. Gale, Phys. Lett. B **584**, 241 (2004)

[22] E. N. E. van Dalen, A. E. L. Dieperink and J. A. Tjon, Phys. Rev. C **67**,065807 (2003).

[23] For all results, we found excellent convergence with partial waves $j, \tilde{j} \leqslant 6$. In addition, we checked that the spin relaxation rate for OPE expanded in partial waves reproduces the analytical result (Eq. (38) in Ref. [10]).